MODELING AND SIMULATION BY LASER AND PLASMA CUTTING OF SOME STEELS AND POLYMERIC MATERIALS

NIȚĂ Liviu-Florinel, POP József[1], RUSU Andrei-Cosmin[1], Liviu Daniel GHICULESCU[2]
[1]Faculty: Industrial Engineering and Robotics, specialization: Machine building Technology, year of study: 2021-2022, e-mail: pop.jozsef99@gmail.com
[2]Faculty of Industrial Engineering and Robotics, Manufacturing Engineering Department, University POLITEHNICA of Bucharest

ABSTRACT: The following work aims to model and simulate laser and plasma cutting of some steel and polymer materials. These types of machining are increasingly used to obtain complex, costly and difficult contours to obtain with current conventional technologies. The Comsol Multiphysics program was used to model with finite elements and to simulate the laser and plasma cutting process of the established materials. After the introduction of the parameters in Comsol Multiphysics and their optimization, experiments were carried out to obtain an optimal cut and some practical tests on the machines specific to each type of materials: stainless steel, steel C45, PVC and plexiglas. These samples were analyzed in terms of cutting quality and implicitly the roughness obtained

KEYWORDS: Laser, plasma, steel, polymeric material, cutting, simulation, optimization

1. Introduction

The process of "light amplification by stimulating emission of radiation" (LASER) is framed in unconventional thermal technologies, but due to its countless applications: electrotechnics, machine building, fine mechanics, aeronautics and due to the reduction of the costs of laser installations, the process tends to become classic. [1]

Laser cutting process is a thermal process in which the laser beam is focused and used to melt the semi-finished material. A coaxial gas jet is used to remove the molten material [2]. In CO2 laser cutting we have a gas mixture that includes carbon dioxide [3].

Plasma cutting is a process in which an inert gas (compressed air) is blown at high speed from a nozzle, at the same time an electric arc is formed by a copper electrode at the nozzle level, converting part of the gas into plasma. Plasma is the fourth state of matter, a gas-like substance being a mixture of electrons, positive ions, and neutral particles (atoms or molecules) that are in continuous and disordered motion. The concentrations of electrons and ions are approximately equal, so macroscopically the plasma is electrically neutral. [4]

In the cutting process, the plasma arc locally melts the material and removes it at high speed, realizing the cutting purpose. The high degree of energy concentration and the high temperature of the arc make it possible to cut metal and metal alloys, high alloy steels, aluminum, copper, titanium.

2. State of the art

Laser cutting is a contact-free thermal processing process with high automation. High dimensional accuracy and low roughness of the processed surface can be obtained.

The high-power density beam when focused on a small, point-sized surface melts and vaporizes the material in a fraction of a second and is removed by a jet of coaxial gas. [5]

In Figure 3. above, 1 is the resonant cavity, 2 is the prism of deflection of the laser beam toward the desired direction; 3 - focus lens (made of NaCl, Ge, CdTe, etc.); 4 – the semi-finished material moving at the speed of v.

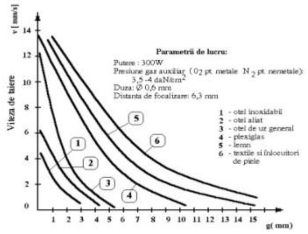

Fig. 1 Working parameters on laser cutting [2]

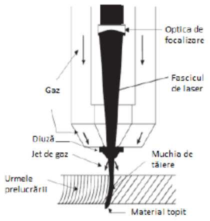

Fig. 2 Laser cutting principle scheme [5]

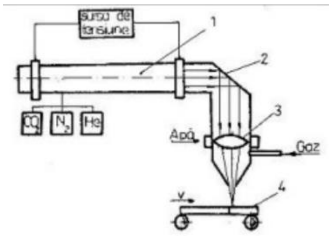

Fig. 3. Components of laser cutting equipment [1]

The laser and plasma cutting process is achieved by automation with CAD/CAM systems, they control either 3-axis flat beds or 6-axis robots for three-dimensional cutting. [5]

From an environmental point of view, it is recommended that laser cutting machines be operated at maximum power and processing speed possible, and from a resource point of view, it is necessary to optimize the cut in order to save raw material, processing time and reduce machine wear. [6]

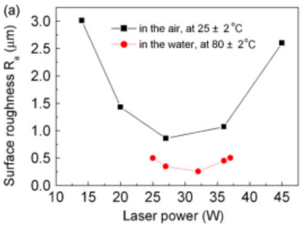

Fig. 4 Roughness according to laser power [11]

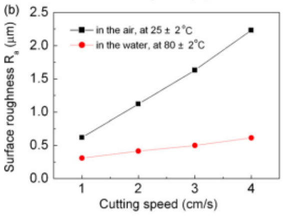

Fig. 5 Roughness according to cutting speed [11]

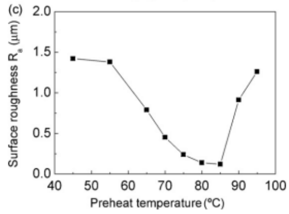

Fig. 6 Influence of material preheating on roughness [11]

Figures 4 and 5 show that it is insufficient to change only certain parameters in order to achieve the best possible roughness. In the case of plexiglass, the lower the cutting speed, the more qualitative the cut is, and therefore the roughness is better.

Table 1. Results obtained when laser cutting of polymeric materials

The material	Laser beam output power, P [kW]	Cutting thickness, h [mm]	Cutting speed, vt [m/min]
Polyvinyl chloride	0.3	3.2	3.6
Plexiglas	0.3	9	2.5

From Table 1 we can see that the parameters used for cutting vary depending on the material. The cutting speed varies depending on the thickness of the material and its characteristics.

In the case of plasma generators using direct current generation, the electric arc is maintained either between the tungsten electrode as cathode and the copper nozzle as anode, or between the electrode and an anode outside the plasma generator (the part).

The plasma cutting nozzle performs the function of creating a high-speed plasma flow. The geometric configuration of the nozzle determines the speed and power of the plasma cutter, as well as the quality of the cut edge obtained. The required pressure is provided by the air compressor. [7]

The cutting speed is inversely proportional to the nozzle diameter. To form a high-quality plasma arc, an air vortex compressed air source is used. [8]

The possibilities of increasing the cutting speed are as follows: increase the intensity of the spring; increase arc tension by using biatomic gases (H2, N2, O2, etc.) [4]

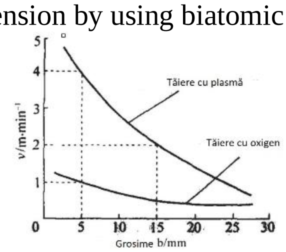

Fig. 8 Variation of plasma velocity according to thickness [10]

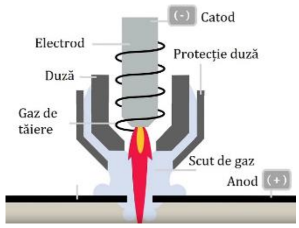

Fig. 9 Plasma cutting principle scheme [9]

3. Experiments

Table 2. Characteristics of the laser cutting machines Bodor i7 1kW and NOVA51

Characteristics	Bodor i7 1kW	NOVA51
Laser source power [W]	1000	100-130
Mode of operation	Continuous/modulated	Continuous/modulated
Wavelength [nm]	1080±10	1080±10
Laser beam quality	≤1.5mm x mrad (50µm QBH)	-
Frequency [kHz]	≤20	≤5
Diameter of optical fiber [µm]	50, doped with ytterbium	-
Laser spot diameter [mm]	Focalization depending on thickness	Focalization depending on thickness
Maximum thickness [mm]	12 (steel)	10 (polymeric materials)

Normal parameters
v=80 mm/s
P=1000 W

Low power
v=80 mm/s
P=800 W

Increased speed
v=90 mm/s
P=1000 W

Low speed
v=70 mm/s
P=1000 W

Fig. 10 Results obtained when laser cutting C45 material according to parameters

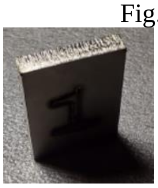

Normal parameters
v=70 mm/s
P=1000 W

Low power
v=70 mm/s
P=800 W

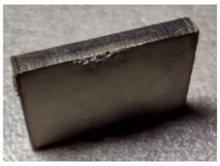

Increased speed
v=80 mm/s
P=1000 W

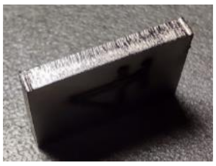

Low speed
v=60 mm/s
P=1000 W

Fig. 11 Results obtained when cutting stainless steel type 304 material according to parameters

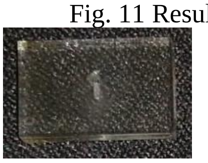

Normal parameters
v=15 mm/s
P=78 W

Low power
v=15 mm/s
P=65 W

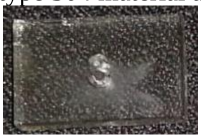

Low speed
v=10 mm/s
P=78 W

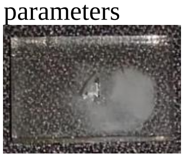

Increased speed
v=17 mm/s
P=78 W

Fig. 12 Results obtained when cutting the plexiglass material according to parameters

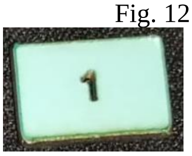

Normal parameters
v=15 mm/s
P=78 W

Low power
v=15 mm/s
P=65 W

Low speed
v=10 mm/s
P=78 W

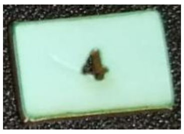

Increased speed
v=17 mm/s
P=78 W

Fig. 13 Results obtained when cutting PVC material according to parameters

Table 4. Features of the Powermax105 SYNC Plasma cutting machine plasma generator

Generator power [kW]	Maximum 30 kW for 105A current
Voltage [V]	380
Current intensity	35 - 105
Gas supply	Clean, dry air, no oil or oxygen
Optimum intake gas pressure [bar]	7.6–8.3 bar (110–120 psi)
Minimum inlet gas pressure [bar]	4.6 bar (58 psi)
Type of power supply	IGBT Inverter (Bipolar Transistor with isolated deck)

Inox 2mm
v = 4350 mm/min
p = 5 bar
I=35A (P = 13.3 kW)

Inox 4mm
v = 3500 mm/min
p = 5.6 bar
I=45A (P = 17.1 kW)

C45 4mm
v = 3500 mm/min
p = 5.6 bar
I=45A(P = 17.1 kW)

C45 2mm
v = 4350 mm/min
p = 5 bar
I=35A (P = 13.3 kW)

Fig. 14 Cutting results for Inox and C45 according to the parameters specific to each thickness.

4. Modeling and simulation

Figure 15 shows the parameterization of the three models.

Parameters

Name	Expression	Value	Description
W	1e14[W/cm^2]	1E18 W/m^2	
Wp	P/(100*lambda^2)	8.5734E12 W	Densitatea de putere [W/m^2]
ucon	5	5	unghi con de focalizare [grd]
dspotprim	5*lambda	5.4E-6	diametrul spotului minim (teoretic)
lambda	1080e-9	1.08E-6	lungimea de unda [m]
uconrad	(3.14/180)*ucon	0.087222	unghi con de focalizare [rad]
dspot	0.009[mm]	9E-6 m	diametrul spotului laser [um]
gp	2[mm]	0.002 m	grosimea piesei
speed	70[mm/s]	0.07 m/s	viteza de avans [m/s]
tstop	(l1-2*rgaz)/speed	0.085714 s	timp de prelucrare [s]
l1	10[mm]	0.01 m	latime piesa
l2	20[mm]	0.02 m	lungime piesa
rgaz	2[mm]	0.002 m	raza spot gaz
Ttop304	1400+273.15	1673.2	temperatura de topire inox 304
P	1000[W]	1000 W	Putere laser
x0	rgaz	0.002 m	distanta de referinta de la centrul spotului laser
sigma	dspot/6	1.5E-6 m	abaterea medie patratica
A1	0.15	0.15	coeficient de absorbtie in otel
emi	0.9	0.9	coeficient de emisivitate
h1	10[W/(m^2*K)]	10 $W/(m^2 \cdot K)$	coeficient de transfer termic
Ed	P/(pi*0.25*dspot^2)	1.5719E13 W/...	Densitatea de putere pe spotul laser
xr	x0+speed*tp	0.002 m	punctul de referinta mobil
tp	0[s]	0 s	timpul de prelucrare

Laser: steels

Parameters

Name	Expression	Value	Description
W	1e14[W/cm^2]	1E18 W/m^2	
Wp	P/(100*lambda^2)	2.225E9 W	Densitatea de putere [W/m^2]
ucon	5	5	unghi con de focalizare [grd]
dspotprim	5*lambda	5.3E-5	diametrul spotului minim (teoretic)
lambda	10.6e-6	1.06E-5	lungimea de unda [m]
uconrad	(3.14/180)*ucon	0.087222	unghi con de focalizare [rad]
dspot	0.14[mm]	1.4E-4 m	diametrul spotului laser [um]
gp	2[mm]	0.002 m	grosimea piesei
speed	1.500[mm/s]	0.0015 m/s	viteza de avans [m/s]
tstop	(l1-2*rgaz)/speed	6 s	timp de prelucrare [s]
l1	10[mm]	0.01 m	latime piesa
l2	15[mm]	0.015 m	lungime piesa
rgaz	0.5[mm]	5E-4 m	raza spot gaz
TtopPVC	177+273.15+20	470.15	temperatura de topire PVC
P	25[W]	25 W	Putere laser
x0	rgaz	5E-4 m	distanta de referinta de la centrul spotului laser
sigma	dspot/6	2.3333E-5 m	abaterea medie patratica
A1	0.28	0.28	coeficient de absorbtie in plastic
emi	0.91	0.91	coeficient de emisivitate
h1	10[W/(m^2*K)]	10 $W/(m^2 \cdot K)$	coeficient de transfer termic
Ed	P/(pi*0.25*dspot^2)	1.624E9 W/m^2	Densitatea de putere pe spotul laser
xr	x0+speed*tp	5E-4 m	punctul de referinta mobil
tp	0[s]	0 s	timpul de prelucrare

Laser: polymer materials

Parameters

Name	Expression	Value	Description
W	1e14[W/cm^2]	1E18 W/m^2	
Wp	P/(100*lambda^2)	1.2003E14 W	Densitatea de putere [W/m^2]
ucon	5	5	unghi con de focalizare [grd]
dspotprim	5*lambda	5.4E-6	diametrul spotului minim (teoretic)
lambda	1080e-9	1.08E-6	lungimea de unda [m]
uconrad	(3.14/180)*ucon	0.087222	unghi con de focalizare [rad]
dspot	0.2[mm]	2E-4 m	diametrul spotului laser [um]
gp	2[mm]	0.002 m	grosimea piesei
speed	5[m/min]	0.083333 m/s	viteza de avans [m/s]
tstop	(l1-2*0.2*rgaz)/speed	0.1104 s	timp de prelucrare [s]
l1	10[mm]	0.01 m	latime piesa
l2	20[mm]	0.02 m	lungime piesa
rgaz	2[mm]	0.002 m	raza spot gaz
Ttop304	1400+273.15	1673.2	temperatura de topire inox 304
P	14000[W]	14000 W	Putere laser
x0	rmgaz+dspot/2	2E-4 m	distanta de referinta de la centrul spotului
sigma	dspot/6	3.3333E-5 m	abaterea medie patratica
A1	0.56	0.56	coeficient de absorbtie in otel
emi	0.25	0.25	coeficient de emisivitate
h1	10[W/(m^2*K)]	10 $W/(m^2 \cdot K)$	coeficient de transfer termic
Ed	P/(pi*0.25*dspot^2)	4.4563E11 W/...	Densitatea de putere pe spotul laser
xr	x0+speed*tp	2E-4 m	punctul de referinta mobil
tp	0[s]	0 s	timpul de prelucrare
rmgaz	0.1[mm]	1E-4 m	raza margine gaz_plasma

Plasma: steels

Fig. 15 Parameters used in modeling and simulation

Figure 16 shows how the variables were set, they are common to the three models. The distribution of energy on the laser spot and plasma follows Gauss's curve.

Variables

Name	Expression	Unit	Description
G_space	exp(-(x-xr)^2/(2*sigma^2))		
Plaser	A1*Ed	W/m^2	
LHS	Plaser*G_space	W/m^2	

Fig. 16 Definition of variables

Figure 18 shows the characteristics of the materials used

Property	Variable	Value	Unit
Thermal conductivity	k_iso ; kii = k_iso, kij = 0	16.2	W/(m·K)
Density	rho	8000	kg/m^3
Heat capacity at constant pressure	Cp	502	J/(kg·K)

304 Stainless steel

Property	Variable	Value	Unit
Heat capacity at constant pressure	Cp	475[J/(kg*K)]	J/(kg·K)
Density	rho	7850[kg/m^3]	kg/m^3
Thermal conductivity	k_iso ; kii = k_iso, kij = 0	44.5[W/(m*K)]	W/(m·K)

Steel C45

Property	Variable	Value	Unit
Density	rho	1760[kg/m^3]	kg/m^3
Thermal conductivity	k_iso ; kii = k_iso, kij = 0	0.1[W/(m*K)]	W/(m·K)
Heat capacity at constant pressure	Cp	880	J/(kg·K)

PVC

Property	Variable	Value	Unit
Density	rho	1180[kg/m^3]	kg/m^3
Thermal conductivity	k_iso ; kii = k_iso, kij = 0	0.18[W/(m*K)]	W/(m·K)
Heat capacity at constant pressure	Cp	1700	J/(kg·K)

Plexiglas

Fig. 18 Material characteristics

Figure 19 shows boundary conditions

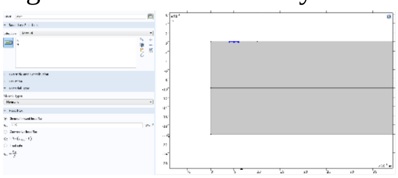

Laser

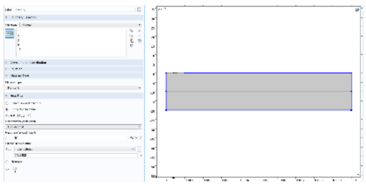

Cooling

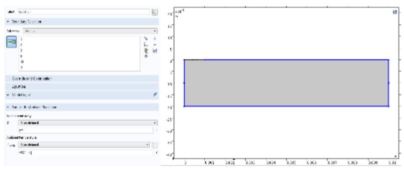

Radiation

Fig. 19 conditions at the limit

The mesh consists of forming a network of triangles, and the calculation of the temperature distribution is obtained based on the approximation with the values in the peaks of each triangle. The smaller the triangles (fine) the better the accuracy. The exception to this step is the model developed for polymeric materials,

because it is very sensitive to changing parameters and implicitly to obtaining optimal results, it was considered a solution to create an extra-fine mesh on all surfaces that will give us a better result.
The two layers (Figure 20 c) are created in order to help in future steps, namely in creating the mesh. Thus on the upper section will be a finer mesh (extra fine), and on the lower section a less fine mesh.

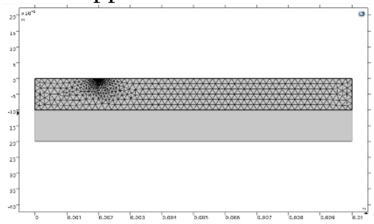
A) creating the network on the top section

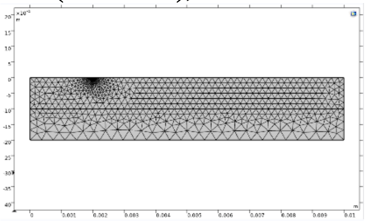
B) creating the network on the lower section

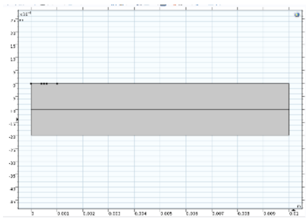
c) creation of layers

Fig. 20 Creation of the mesh

In order to simulate the movement of the laser/plasma spot on the surface of the blank, the parametric sweep option (figure 21 a) was used with the sweep processing time (t_p) parameter. The time-dependent parameter was also set as the final processing time, t_{stop} (Figure 21 b)

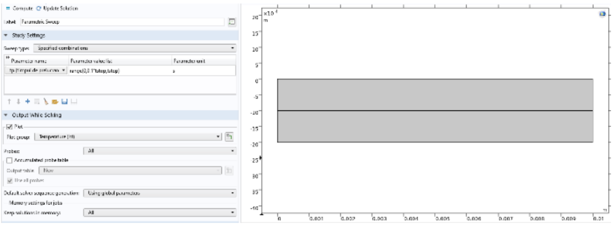
a) Parametric Sweep

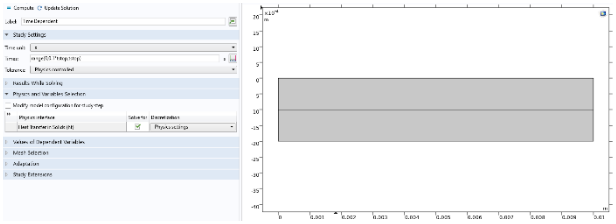
b) Time dependent

Fig. 21 Settings for performing the study

Table 11 shows the results obtained when simulating cuts by varying the speed, spot diameter and laser power (when cutting polymeric materials) achieving three situations: Moderate heating (low roughness), overheating (high roughness) and low heating (high roughness with the appearance of striations).

Table 11. Results obtained in Comsol Multiphysics for laser/plasma cutting of steel and polymeric materials

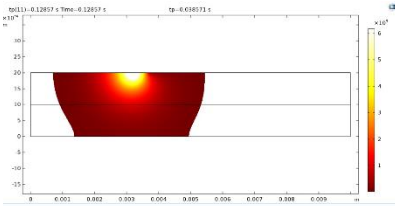
Optimal laser cutting: Stainless steel
spot diameter=0,015 mm
cutting speed=70 mm/s

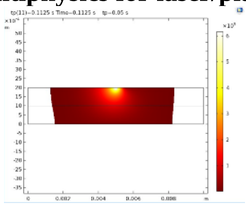
Optimal laser cutting: C45
spot diameter=0,012 mm
cutting speed=90 mm/s

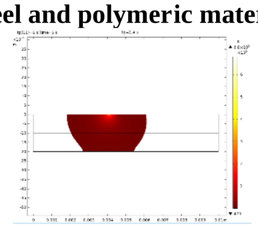
Optimal laser cutting: PVC
spot diameter=0.14 mm
cutting speed=1.5 mm/s
Power = 25 W

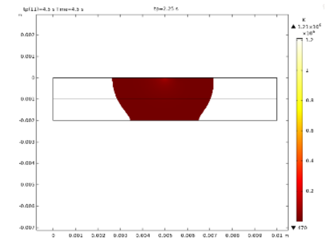
Optimal laser cutting: Plexiglas
spot diameter=0.2 mm
cutting speed=2 mm/s
Power=30 W

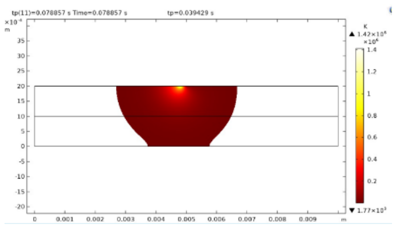
Optimal plasma cutting: Stainless steel
spot diameter=0,2 mm
cutting speed=7000mm/min.

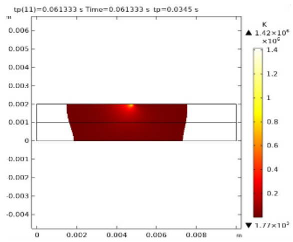
Optimal plasma cutting: C45
spot diameter=0,1 mm
cutting speed=9000mm/min.

5. Conclusions

Finite element modeling and simulations of laser and plasma cutting processes of stainless steel 304, C45 steel, as well as laser cutting of PVC and plexiglass polymer materials were made. The models created are dynamic by scenting the processing time to simulate the speed of advance of the laser/plasma spot. The contribution to the heating of the material (temperature distribution within the semi-finished) of the following technological parameters was highlighted, aiming to reduce the roughness of the processed surface, increasing the quality of the surface layer. The analyzed technological parameters were: Laser/plasma spot diameter, advance speed and power distributed on the laser/plasma spot. An optimization was achieved in terms of material heating by correlating the three parameters mentioned. Experiments were also carried out on laser and plasma cutting of the mentioned materials, which confirmed the influence of the mentioned technological parameters on the quality of the processed surfaces.

6. Bibliography

[1]. Ghiculescu, D. (2020), Curs Tehnologii Neconvenționale, București.
[2]. Marinescu, N.I., Ghiculescu, D. (2017), *Procese tehnologice cu fascicule, oscilații și jeturi*, editura Printech, București
[3]. Landry, J. (2020, 26 november)., “FIBER LASERS: EVERYTHING YOU NEED TO KNOW”. Available at: https://www.laserax.com/blog/fiber-laser . Accessed: 25.04.2022
[4]. Amza, Gh. (2009),– *Tehnologia Materialelor si produselor*, vol 3, editura Printech, Bucuresti.
[5]. V.Senthil Kumar and Dr.G.Jayaprakash (2017), “State of Art of Laser Cutting Process”, International Journal for Modern Trends in Science and Technology.
[6]. M. Radovanovic and P. Dasic (2006), “Research on surface roughness by laser cut, ”*The Annals of University Dunarea de Jos of Galati Fascicule VIII, Tribology*
[7]. K. Küpfmuller, W. Fathis und A. Reibiger (2013), TheoretischeElektrotechnik: Eine Einführung, Springer
[8]. H. Zohm (2013), Plasmaphysik, LMU München, München
[9] ***Hypertherm, „Plasma cutter technology”. Available at: https://www.hypertherm.com/learn/cutting-education/plasma-technology/ . Accessed: 02.05.2022
[10] „Huafei” (2020, 19 november), „oxy-fuel flame cutting VS plasma cutting”. Available at: https://thebestcnc.com/oxy-fuel-cutting-vs-plasma-cutting/ . Accessed: 02.05.2022
[11] Yongguang H., Shibing L., (2009), “Surface roughness analysis and improvement of PMMA-based microfluidic chip chambers by CO_2 laser cutting”. Available at: https://www.sciencedirect.com/science/article/pii/S0169433209013993?casa_token=AWDY3vreYlMAAAAA:MgwjcfndeVx6yri3hOVIR3L-8DxIyYHmgkUbFX1iKnzmVrrtXiQx9UXTxjkUI-PBRsBqQLBmpeo . Accessed: 04.05.2022